Electronic Supplementary Material (ESI) for Journal of Materials Chemistry A.

Highly sensitive omnidirectional signals manipulation from flexible anisotropic strain sensor based on aligned carbon hybrid nanofibers

Yunfeng Hu,[a] Tieqi Huang,[a] Huijuan Lin,[a] Longwei Ke,[a] Wei Cao,[a] Chen Chen,[b] Wenqing Wang,[a] Kun Rui[a] and Jixin Zhu*[a]

[a] Key Laboratory of Flexible Electronics (KLOFE) & Institute of Advanced Materials (IAM), Nanjing Tech University (Nanjing Tech), 30 South Puzhu Road, Nanjing 211816, P. R. China

[b] Hangzhou Gaoxi Technology Co, Ltd, 6 Naxian Street, Hangzhou 311100, Zhejiang, China

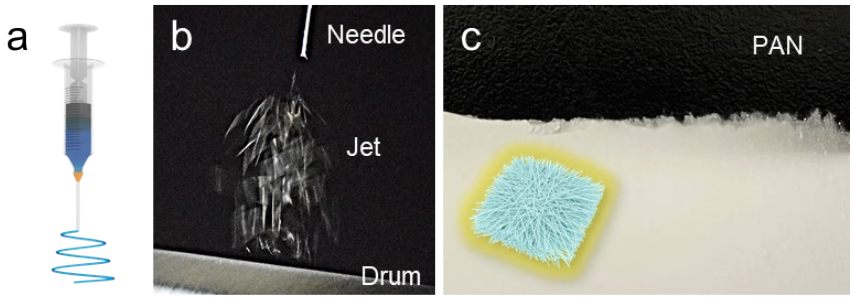

Fig S1. (a) Schematic and (b) photograph of the liquid jets produced during electrospinning of 10 wt% PAN solution. (c) Photograph and schematic diagram of electrospun PAN film.

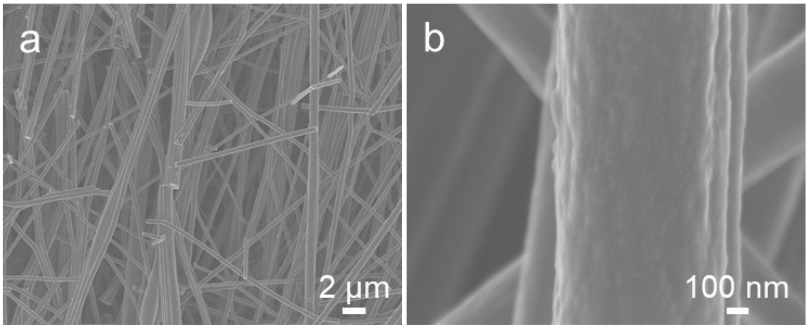

Fig S2. FE-SEM images of VN/ACNF-1.

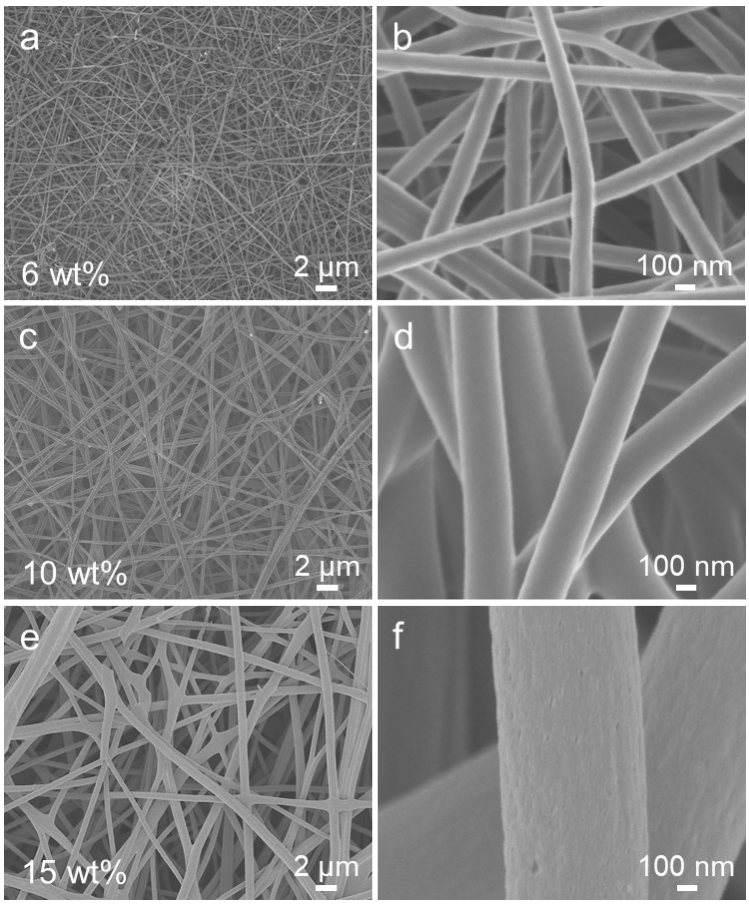

Fig S3. FE-SEM images of CNF obtained by different PAN electrospinning precursor solution concentrations of (a, b) 6 wt%, (c, d) 10 wt% and (e, f) 15 wt%.

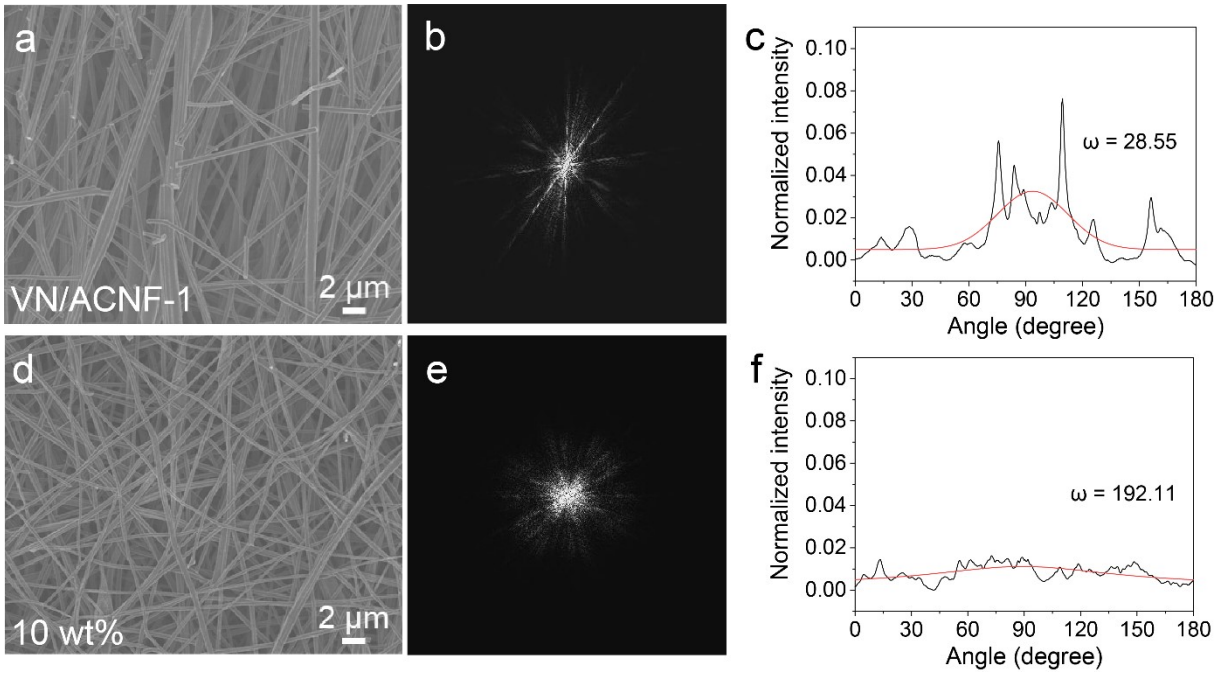

Fig S4. Characterization of the degree of alignment. (a) FE-SEM image, (b) FFT output image. (c) Pixel intensity plots versus detection angle and angular analysis fitted with the Cauchy-Lorentz distribution for VN/ACNF-1. (d) FE-SEM image, (e) FFT output image. (f) Pixel intensity plots versus detection angle and angular analysis fitted with the Cauchy-Lorentz distribution for CNF obtained from solution concentration of 10 wt%. The image processing process was carried out with ImageJ software supported by an oval profile plugin. The distribution intensity images were fitted using the Cauchy-Lorentz distribution function:

$$y = y_0 + \frac{2A}{\pi}\left(\frac{\omega}{4(x - x_0)^2 + \omega^2}\right)$$

The location parameter, x_0, indicates the angle corresponding to the peak of the curve. The scale parameter, ω, specifies the half-width at half-maximum (HWHM), which presents the angle of deviation from the principle orientation and thus measures the degree of alignment.

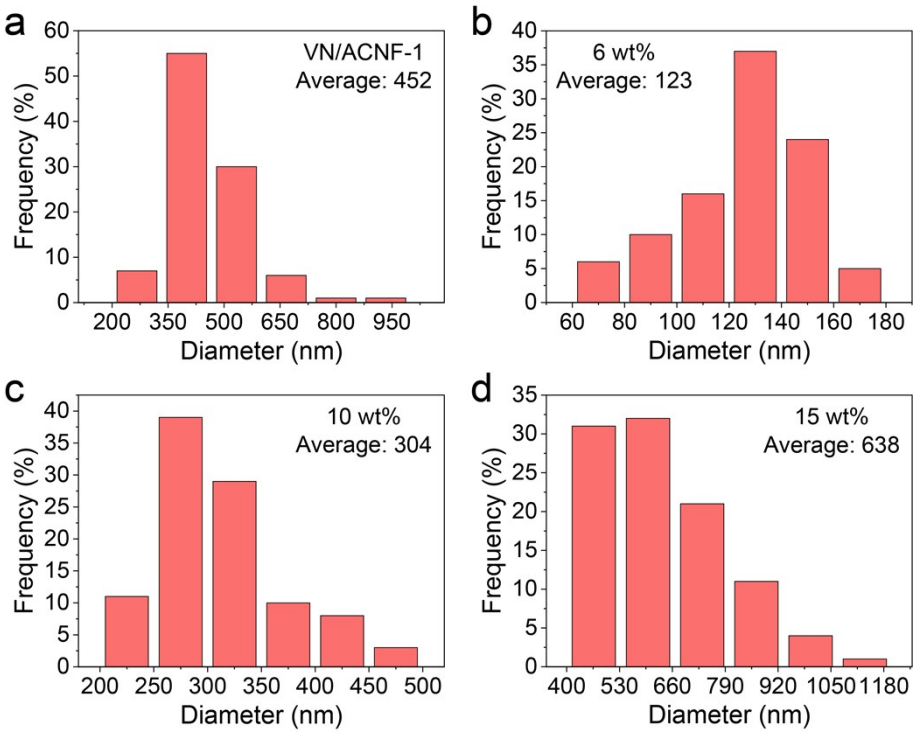

Fig S5. The fiber diameter distribution of (a) VN/ACNF-1and CNF obtained by different PAN electrospinning precursor solution concentrations of (b) 6 wt%, (c) 10 wt%, (d) 15 wt%.

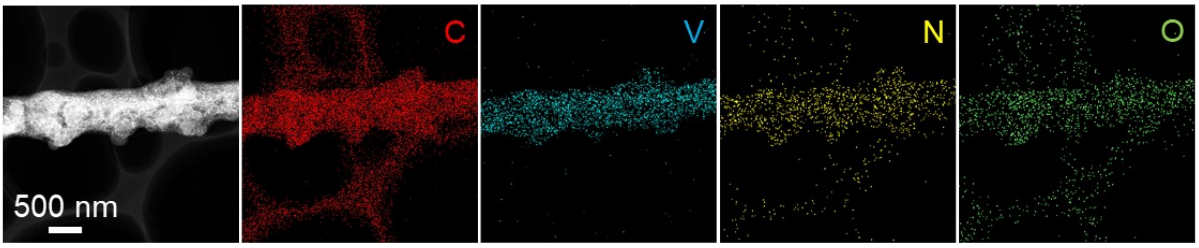

Fig S6. Dark field TEM image of VN/ACNF-2 fiber and the corresponding EDS elemental mapping images.

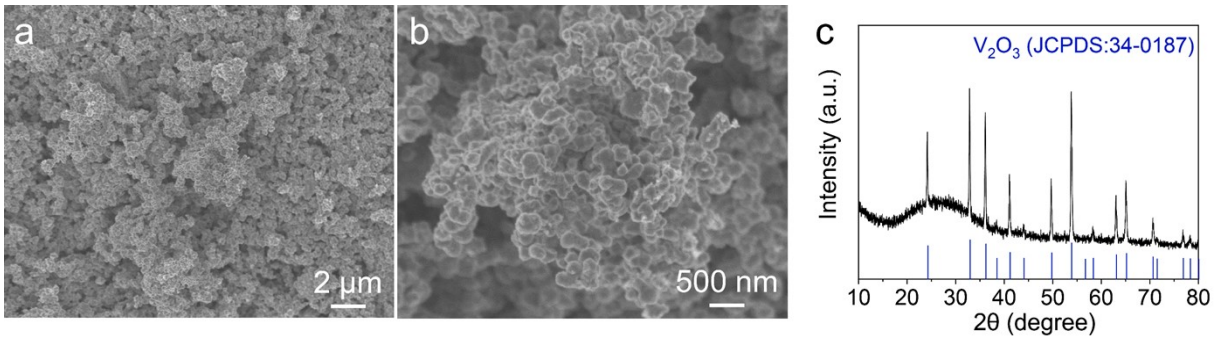

Fig S7. (a, b) FE-SEM images and (c) XRD pattern of heating $VO(acac)_2$ powder without adding PAN at 900 °C for 2 h in N_2 atmosphere.

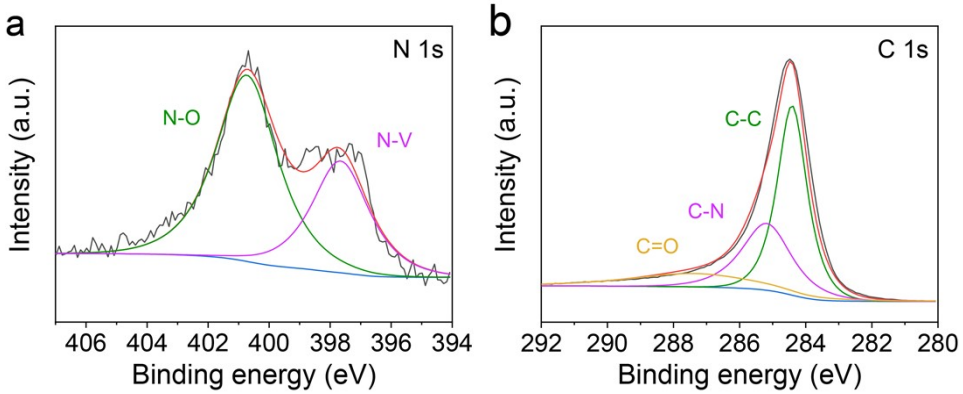

Fig S8. XPS deconvolutions of (a) N 1s and (b) C 1s in VN/ACNF.

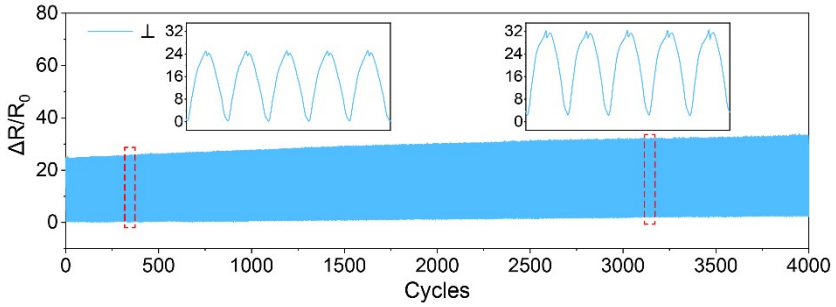

Fig S9. The durability tests of strain sensor at a strain of 70% in the ⊥ direction for 4000 cycles.

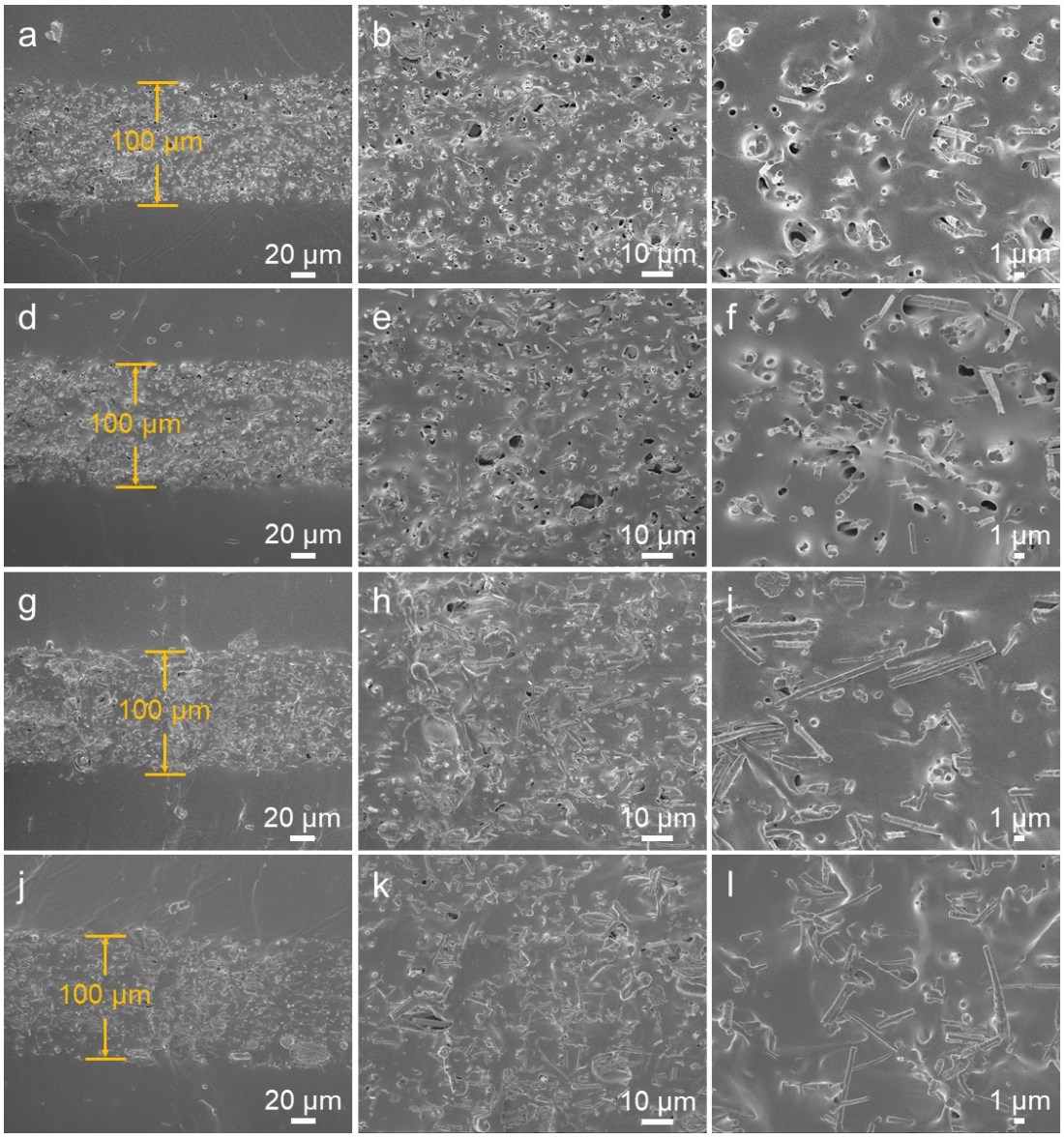

Fig S10. Cross-sectional FE-SEM images of the sensor in (a-c) original state, (d-f) after cycling for 4000 times in the $\parallel$ direction; and (g-i) original state, (j-l) after cycling for 4000 times in the $\perp$ direction.

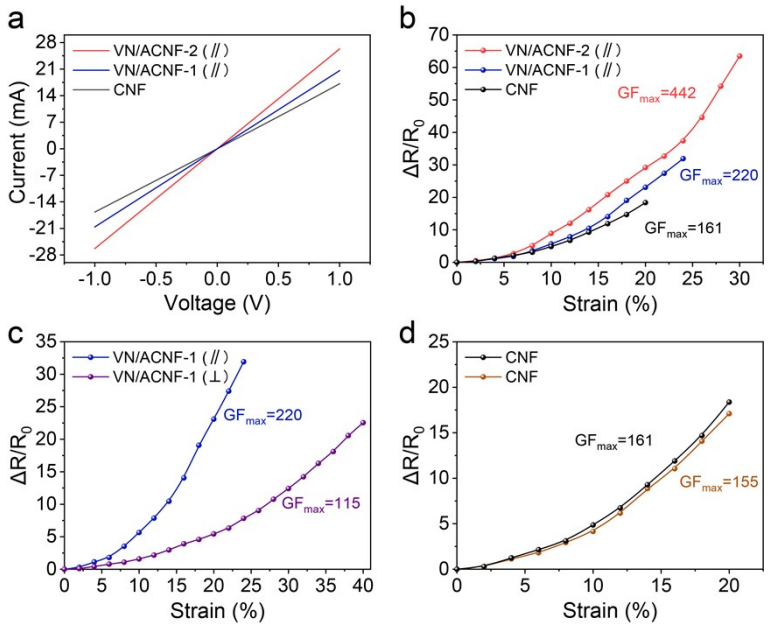

Fig S11. (a) *I-V* curves of the sensor assembled by different nanofibers films. (b) Relative resistance change as a function of strain for CNF, VN/ACNF-1 and VN/ACNF-2 sensors. (c) Relative resistance change of VN/ACNF-1 sensor as a function of strains in ∥ and ⊥ directions. (d) Relative resistance change of CNF sensor as a function of strains in two directions.

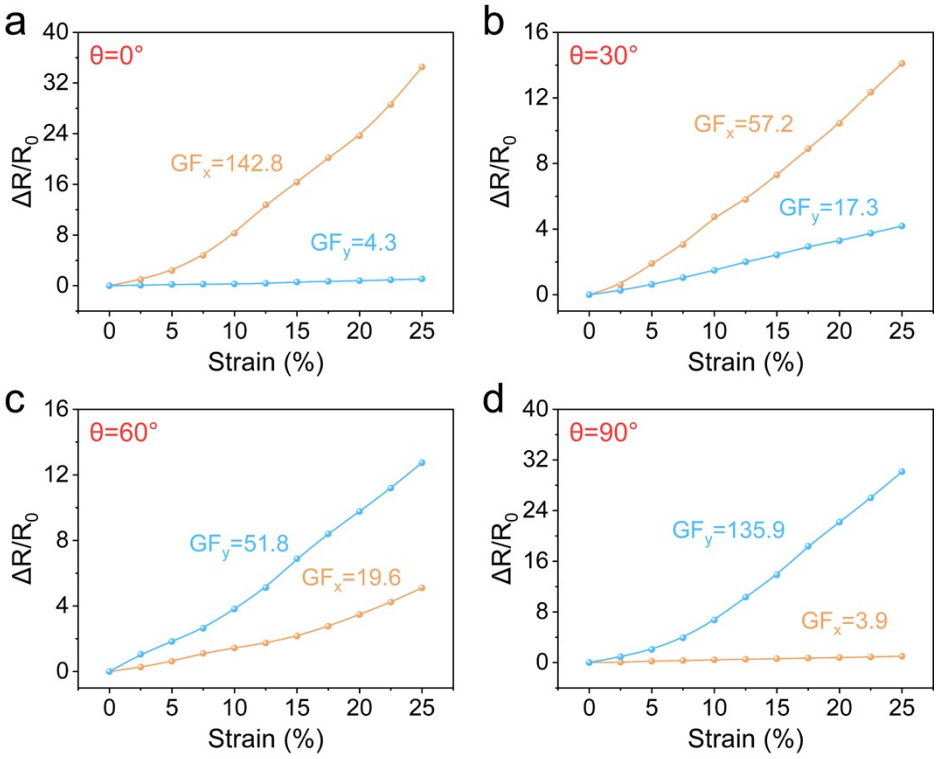

Fig S12. Directional sensing performance of cross-shape structure multidirectional sensor under different stretching directions of θ = (a) 0°, (b) 30°, (c) 60° and (d) 90°.

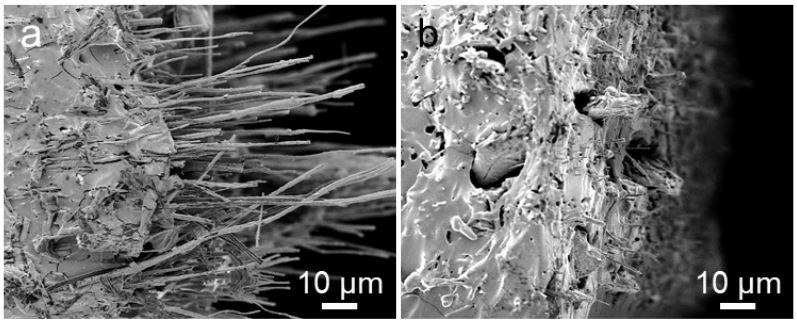

Fig S13. Cross-sectional FE-SEM images of the sensor after being stretched until fracture in the (a) ∥ direction and (b) ⊥ direction.

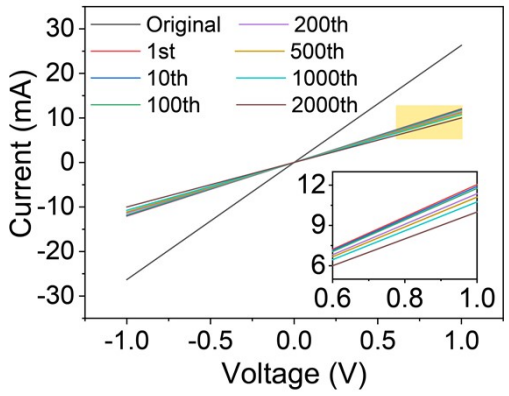

Fig S14. *I*–*V* curves of the VN/ACNF-2 sensor in the ∥ direction measured at original and after each loading state.

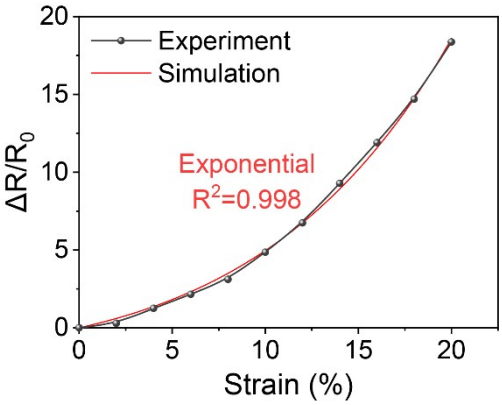

Fig S15. Response of CNF sensor to the applied strain by experimental measurement and numerical simulation.

Table S1. Comparison of viscosity and conductivity of different electrospinning precursor solution.

Precursor solution	Conductivity/ μS cm^{-1}	Viscosity/ cps
10 wt% PAN	93	686
0.2 g $VO(acac)_2$ + 0.25 g $H_2C_2O_4$ + 10 wt% PAN	127	790

Table S2. Comparison of the sensing performance of VN/ACNF-2 strain sensor with the previous anisotropic strain sensors.

Materials	Maximum strain (%)	Maximum GF	Selectivity	Ref.
VN/ACNF-2	**70**	**442**	**2.95**	**This work**
ACNF/PDMS	30	180	3.33	1
Vertical graphene/PDMS	10	10.28	0.14	2
Microstructured AgNW-sarrayed surface	150	24.6	0.34	3
AgNWs fiber electrodes/polymer matrix	30	3.2	0.09	4
Cellulose nanofiber-CNT hybrid aerogels	9	1.19	0.026	5
AgNWs/stiffness-variant substrate	60	21.1	0.5	6
Pre-strained AgNW/PDMS	35	20	0.48	7
Wrinkled and cracked CNT/GO/VHB	100	287.6	6.3	8
Aligned SWCNT/PDMS	16	59	1.29	9
Anisotropic graphene/PDMS	120	27	0.11-0.44	10

Table S3. Comparison of conductivity of CNF, VN/ACNF-1 and VN/ACNF-2 films.

Sample	**Conductivity/ S m^{-1}**
CNF	18.5
VN/ACNF-1	28.1
VN/ACNF-2	35.8

References

1 J. H. Lee, J. Kim, D. Liu, F. Guo, X. Shen, Q. Zheng, S. Jeon and J. K. Kim, *Adv. Funct. Mater.*, 2019, **29**, 1901623.

2 S. Huang, G. He, C. Yang, J. Wu, C. Guo, T. Hang, B. Li, C. Yang, D. Liu, H. J. Chen, Q. Wu, X. Gui, S. Deng, Y. Zhang, F. Liu and X. Xie, *ACS Appl. Mater. Interfaces*, 2019, **11**, 1294-1302.

3 K. H. Kim, N. S. Jang, S. H. Ha, J. H. Cho and J. M. Kim, *Small*, 2018, **14**, e1704232.

4 Y. Cheng, R. Wang, H. Zhai and J. Sun, *Nanoscale*, 2017, **9**, 3834-3842.

5 C. Wang, Z. Z. Pan, W. Lv, B. Liu, J. Wei, X. Lv, Y. Luo, H. Nishihara and Q. H. Yang, *Small*, 2019, **15**, e1805363.

6 S. H. Ha, S. H. Ha, M. B. Jeon, J. H. Cho and J. M. Kim, *Nanoscale*, 2018, **10**, 5105-5113.

7 K. K. Kim, S. Hong, H. M. Cho, J. Lee, Y. D. Suh, J. Ham and S. H. Ko, *Nano Lett.*, 2015, **15**, 5240-5247.

8 H. Zhang, D. Liu, J.-H. Lee, H. Chen, E. Kim, X. Shen, Q. Zheng, J. Yang and J.-K. Kim, *Nano-Micro Lett.*, 2021, **13**, 122.

9 C. Sui, Y. Yang, R. J. Headrick, Z. Pan, J. Wu, J. Zhang, S. Jia, X. Li, W. Gao, O. S. Dewey, C. Wang, X. He, J. Kono, M. Pasquali and J. Lou, *Nanoscale*, 2018, **10**, 14938-14946.

10 Z. Zeng, S. I. Seyed Shahabadi, B. Che, Y. Zhang, C. Zhao and X. Lu, *Nanoscale*, 2017, **9**, 17396-17404.